JOURNAL OF SOLID STATE CHEMISTRY 105, 399–405 (1993)

Crystal Chemistry and Magnetic Properties of the Ternary Compounds $RE_3Ag_xGa_{11-x}$ (RE = Y, Gd, Tb, Dy, Ho, Er, Tm, and Yb)

YU. N. GRIN* AND M. ELLNER

Max-Planck-Institut für Metallforschung, Institut für Werkstoffwissenschaft, D-7000 Stuttgart, Seestrasse 75, Germany

K. HIEBL AND P. ROGL

Institut für Physikalische Chemie der Universität Wien, A-1090 Wien, Währingerstrasse 42, Austria

AND O. M. SICHEVICH AND O. M. MYAKUSH

Institute of Inorganic Chemistry, University of Lviv, 290005-Lviv, Lomonosov Street 6, Ukraine

Received October 19, 1992; accepted December 10, 1992

Ternary samples with the composition $RE_3Ag_xGa_{11-x}$, RE = Y, Gd, Tb, Dy, Ho, Er, Tm, and Yb, have been synthesized from the elements by arc- or HF-melting and annealing at 600°C. In all cases isotypy with the La_3Al_{11}-type has been confirmed from X-ray powder data. The homogeneity region of the $Yb_3Ag_xGa_{11-x}$ phase has been established by X-ray powder diffraction analysis and ranges at 600°C from $x = 2.6$ to $x = 3.8$. Unit cell parameters in this region reveal a remarkable positive deviation from Vegard's rule corresponding with a partial composition-dependent atomic ordering in the various sites of the La_3Al_{11}-type structure. The occupation mode in the Yb-containing alloys has been studied in detail by full profile X-ray powder analysis for compositions $x = 2.55$ and 3.65 and by X-ray single crystal counter data refinement for the alloy with $x = 3.0$, confirming in all cases full consistency with the La_3Al_{11}-type structure with the space group $Immm$. Throughout the homogeneous range Ag was observed to preferentially occupy the (2c) sites. The relative increase of the Ag occupancy in (2c) with increasing content of silver, however, decreases and for compositions $x > 3.0$, Ag was found to enter the (8l) positions. In correspondence with magnetic susceptibility measurements the peculiar lattice parameter variation observed is due to this complicated mode of Ga/Ag-substitution rather than to a valence change on the ytterbium atom. Magnetic susceptibilities were determined over a temperature range from 4 to 550 K. Above LNT, magnetic behavior of Gd ($x = 2.8$), Tb, Dy, Ho, Er, and Tm compounds ($x = 3.8$) corresponds to the paramagnetism of ideal tripositive rare earth elements. Below $T = 25$ K antiferromagnetic ordering of the RE-moments is encountered for the $Yb_3Ag_xGa_{11-x}$ alloys. The Yb-atom was found to be in a nonmagnetic Yb^{2+} ground state throughout the entire homogeneous range. The susceptibilities are practically temperature independent paramagnetic down to 20 K. $Y_3Ag_3Ga_8$ is a diamagnet.

Introduction

Due to the rather small energy involved in the valence change from Yb^{2+} to Yb^{3+}, intermetallic ytterbium-containing compounds frequently display valence instabilities or valence transitions as a function of temperature and/or composition (*1*).

In a continuation of our systematic studies (*2*, *3*) concerning the formation of compounds with the $BaAl_4$-type and its derivatives in the ternary systems RE–M–Ga, where RE is a rare earth element and M is

* Alexander von Humboldt fellowship, on leave from the Institute of Inorganic Chemistry, University of Lviv.

0022-4596/93 $5.00

one of the platinum group elements or one of the first main group metals, we focus herein on combinations with the heavy rare earth elements with special emphasis on the formation and the magnetic properties of ytterbium compounds. Where the early rare earth members with Ag and Ga were found to crystallize with the $BaAl_4$-type or its deformation variants (*2, 3*), combinations with the late rare earths were recently reported (*4, 5*) to adopt the La_3Al_{11}-type in close relation to the $BaAl_4$ parent type. Details of their structural behavior and magnetism have not been investigated so far and thus became the subject of the present work.

Experimental Details

All samples except the ytterbium compounds, each with a total mass of about 1 g, were prepared by arc melting from ingots of the elements. The ytterbium-containing alloys were synthesized in tantalum crucibles using a high frequency furnace. Weight losses have been checked to be within 1.0 mass%. Homogenization heat treatment at 600°C has been performed on samples wrapped in molybdenum foil, sealed in evacuated silica tubes for 300 h followed by quenching in cold water.

X-ray phase analysis was performed employing Enraf–Nonius Guinier cameras and monochromatized Cu$K\alpha$ radiation. The crystal structures were investigated by single crystal refinement of four-circle diffractometer data collected with Mo$K\alpha$ radiation on a Syntex Pl or by full profile powder data refinement (Siemens D5000 powder diffractometer, Cu$K\alpha$). Crystallographic calculations were performed using the program package CSD (*6*).

Magnetic susceptibility measurements were carried out on a compensated Faraday magnetometer (80 to 550 K) and ac susceptibilities were obtained on a Lake Shore susceptometer (4 to 200 K, ac field = 796 A/m, 133.3 Hz).

Results and Discussion

Crystal Chemistry

X-ray powder patterns of alloys $RE_3Ag_xGa_{11-x}$ confirmed earlier reports of the existence of La_3Al_{11}-type compounds with RE = Gd, Tb, Dy, Ho, Er, Tm, and Yb. A new compound with the La_3Al_{11}-type structure was found in the system with yttrium at the composition $Y_3Ag_3Ga_8$. However, the isotypic Lu-containing compound could not be synthesized. In all cases investigated, Guinier photographs were indexed completely on the basis of a body-centered orthorhombic unit cell (Table I) and X-ray powder intensities confirm isotypy with the La_3Al_{11}-type. The homogeneity range at 600°C was studied in detail for the ytterbium alloys by X-ray powder analysis and was found to extend from $x = 2.6$ to $x = 3.8$ (see Table I). The unit cell dimensions plotted as a function of the silver content are shown in Fig. 1 and reveal a maximum in the c-parameter at $x = 3.2$, whereas the parameters a and b as well as the unit cell volume exhibit a slightly negative deviation from Vegard's rule. In order to reveal the origin of this peculiar behavior, the crystal structure and the atom distribution were studied in detail for the samples with $x = 2.5$, 3.0, and 3.65.

Despite the fact that the alloy composition with $x = 2.5$ is slightly beyond the homogeneity region (see Fig. 1), the small amount of secondary phase allowed a full profile powder analysis after the elimination of several weak peaks of the second phase. The results of the structure refinement using X-ray intensities within 2θ of 15° to 100° (Cu$K\alpha$ radiation) are presented in Table II. Besides a full occupation of the (4j) positions the silver atoms were found to occupy the (2c) sites preferentially.

A single crystal with prismatic shape and suitable for structure investigation could be obtained from the alloy matrix of a sample with the nominal composition $Yb_3Ag_3Ga_8$. X-ray rotation and Weissenberg photographs confirmed the orthorhombic Laue

TABLE I

CRYSTALLOGRAPHIC AND MAGNETIC DATA FOR $RE_3Ag_xGa_{11-x}$ COMPOUNDS

Composition	a (Å)	b (Å)	c (Å)	V (Å^3)	T_N (K)	Θ_p (K)	$\mu_{eff/exp}$ (μ_B)	$\mu_{eff/theor}$ (μ_B)
$Y_3Ag_{3.0}Ga_{8.0}$	4.3034(5)	12.802(2)	9.522(1)	524.6(2)	—	[a]	[a]	[a]
$Gd_3Ag_{2.8}Ga_{8.2}$	4.3190(7)	12.958(3)	9.524(2)	533.0(3)	20	−6.5	8.0	7.94
$Tb_3Ag_{3.8}Ga_{7.2}$	4.3263(6)	12.905(2)	9.524(1)	531.7(2)	23	−2.9	10.0	9.72
$Dy_3Ag_{3.8}Ga_{7.2}$	4.3126(9)	12.835(3)	9.528(2)	527.4(3)	22	5.1	10.7	10.65
$Ho_3Ag_{3.8}Ga_{7.2}$	4.3054(6)	12.806(2)	9.528(1)	525.3(2)	12	−3.1	10.9	10.61
$Er_3Ag_{3.8}Ga_{7.2}$	4.3001(9)	12.766(2)	9.530(2)	523.2(3)	<5	−3.8	9.9	9.58
$Yb_3Ag_{2.5}Ga_{8.5}$	4.3263(6)	12.854(2)	9.662(2)	537.3(3)	[b]	[b]	[b]	[b]
$Yb_3Ag_{2.9}Ga_{8.1}$	4.3283(6)	12.853(1)	9.686(1)	538.6(2)	[b]	[b]	[b]	[b]
$Yb_3Ag_{3.2}Ga_{7.8}$	4.3285(6)	12.846(2)	9.703(2)	539.5(3)	[b]	[b]	[b]	[b]
$Yb_3Ag_{3.5}Ga_{7.5}$	4.3357(7)	12.868(2)	9.676(2)	539.8(3)	[b]	[b]	[b]	[b]
$Yb_3Ag_{3.65}Ga_{7.35}$	4.3603(6)	12.910(2)	9.642(1)	542.8(3)	[b]	[b]	[b]	[b]
$Yb_3Ag_{3.8}Ga_{7.2}$	4.3675(8)	12.937(2)	9.630(2)	544.1(3)	[b]	[b]	[b]	[b]
$Yb_3Ag_{4.2}Ga_{6.8}$	4.3674(9)	12.921(3)	9.626(2)	543.2(3)	[b]	[b]	[b]	[b]
$Tm_3Ag_{3.8}Ga_{7.2}$	4.2858(6)	12.715(2)	9.526(1)	519.1(2)	<5	−0.8	7.7	7.56

[a] Magnetic susceptibility is practically temperature independent in range 80–350 K (-1.2×10^{-4} cm^3/mole).
[b] Temperature independent paramagnetism of Yb^{2+} state.

symmetry *mmm*. No significant indications for superstructure formation could be found. The lattice parameters and extinctions observed were fully compatible with the La_3Al_{11}-type structure. The structure refinement has been performed in space group *Immm* using isotropic extinction and anisotropic thermal parameters and unambiguously revealed the atom order as derived in Table II. Attempts to refine the structure in the noncentrosymmetric space group *Imm*2 (in different setting) had no significant influence on the *R*-value obtained. The silver atoms at this composition again show a full occupation of the (4j) sites and a preferential occupation of the (2c) sites but the Ag-occupancy in (2c) is larger than in case of $x = 2.5$.

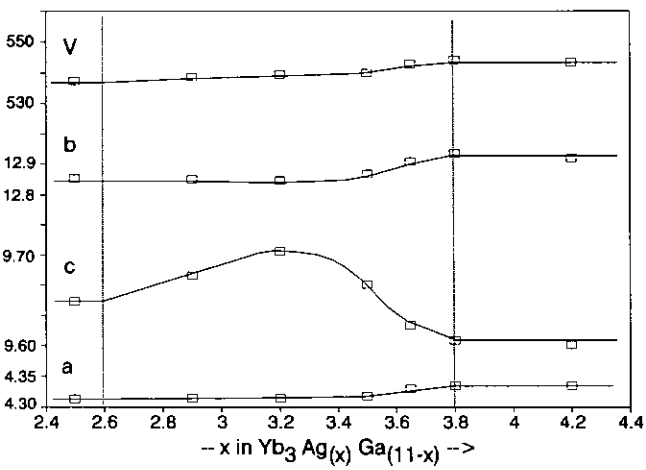

FIG. 1. Unit cell dimensions of $Yb_3Ag_xGa_{11-x}$ alloys versus concentration; the homogeneous range is indicated by vertical bars.

TABLE II

STRUCTURAL DATA OF $Yb_3Ag_xGa_{11-x}$ (La_3Al_{11} STRUCTURE TYPE, SPACE GROUP *Immm*)

x	2.5	3.0	3.65
a,Å	4.3263(6)	4.3284(9)	4.3603(6)
b,Å	12.854(2)	12.860(2)	12.910(2)
c,Å	9.662(2)	9.709(2)	9.642(1)
	4Yb1 ($R1$) in 4(g) 0y0		
y	0.2987(2)	0.29974(6)	0.2994(2)
B	0.72(8)	0.85(2)	0.30(9)
	2Yb2 ($R2$) in 2(a) 000		
B	0.86(11)	0.92(3)	0.28(13)
	8$X1$ in 8(l) 0yz		
$X1$	Ga	Ga	Ga
y	0.3428(4)	0.3412(1)	0.3420(4)
z	0.3689(5)	0.3683(2)	0.3640(6)
B	1.42(13)	0.98(3)	1.6(2)
	8$X2$ In 8(l) 0yz		
$X2$	Ga	Ga	0.90(2)Ga + + 0.10(2) Ag
y	0.1419(4)	0.1424(1)	0.1371(4)
z	0.2816(5)	0.2800(2)	0.2762(7)
B	1.31(13)	0.94(3)	1.5(2)
	4$X3$ in 4(j) $\frac{1}{2}0z$		
$X3$	Ag	Ag	Ag
z	0.6883(6)	0.6901(1)	0.6925(6)
B	1.0(2)	1.25(3)	1.12(14)
	2$X4$ in 2(c) $\frac{1}{2}\frac{1}{2}0$		
$X4$	0.53(3) Ga + 0.47(3) Ag	0.28(2) Ga + 0.72(2) Ag	0.19(3) Ga + 0.81(3) Ag
B	1.3(2)	1.35(5)	1.4(2)
Type of data	Powder full profile	Single crystal	Powder full profile
Number of reflections	161	376	176
R(I)	0.0968		0.1007
R(P)	0.1584		0.1856
R(F)		0.0246	
d(Yb1–$X1$),Å	3.097(4)	3.099(2)	3.131(4)
	3.609(5)	3.615(3)	3.553(6)
d(Yb1–$X2$),Å	3.117(4)	3.131(2)	3.175(5)
	3.386(6)	3.388(3)	3.388(6)
d(Yb1–$X3$),Å	3.163(4)	3.168(2)	3.186(5)
d(Yb1–$X4$),Å	3.373(3)	3.364(3)	3.385(3)
d(Yb1–Yb1),Å	4.3263(6)	4.3284(9)	4.3600(2)
d(Yb1–Yb2),Å	3.839(3)	3.855(2)	3.865(3)
d(Yb2–$X1$),Å	3.220(4)	3.238(2)	3.261(4)
d(Yb2–$X2$),Å	3.276(5)	3.278(2)	3.198(6)
d(Yb2–$X3$),Å	3.708(5)	3.706(2)	3.680(5)
d(Yb2–$X4$),Å	4.3263(6)	4.3284(9)	4.3600(2)
d($X1$–$X1$),Å	2.533(7)	2.558(8)	2.622(8)
d($X1$–$X2$),Å	2.614(4)	2.608(2)	2.580(5)
	2.717(8)	2.697(3)	2.777(8)
d($X1$–$X3$),Å	2.670(7)	2.676(3)	2.626(7)
d($X2$–$X2$),Å	3.574(6)	3.561(2)	3.540(8)
	3.648(8)	3.663(3)	3.675(6)
d($X2$–$X3$),Å	2.844(4)	2.850(2)	2.824(4)
d($X2$–$X4$),Å	2.789(5)	2.814(2)	2.791(6)
d($X3$–$X3$),Å	3.639(8)	3.691(3)	3.712(9)
d($X3$–$X4$),Å	2.827(4)	2.844(2)	2.863(4)

Full profile X-ray powder data refinement for the sample with $x = 3.65$ revealed silver atoms now in the (8l) sites in addition to Ag in (4j) and a high amount of Ag in the (2c) sites (see Table II). Maxima and minima of the lattice parameters at $x = 3.2$ under the assumption of a constant Yb-valency are thus due to the nonlinear Ga/Ag-substitution mode in the (2c) and the (8l) sites. When Ag (8l) site occupation starts for compositions richer in Ag than $x = 3.0$, simultaneous Ag (2c) site occupancy with increasing Ag content becomes less than proportional and unit cell parameters depart from linearity.

In all three cases described, the overall number of silver atoms refined per unit cell is generally less than the nominal composition. This fact may be connected with absorption influences on the refinement of the occupation coefficients.

An analysis of the unit cell dimensions of the $RE_3Ag_xGa_{3-x}$ phases in terms of Pearson's nearest neighbor concept (7) was performed at $x = 3.8$ with atomic coordinates taken from the $Yb_3Ag_3Ga_8$ structure and unit cell parameters taken from Table I. The slopes $\Delta(i\text{–}j)$ versus r_R, where $\Delta(i\text{–}j) = r_i + r_j - d_{ij}$, d_{ij} is the interatomic distance between the atoms i and j, and r_i, r_j, and r_R are the atomic radii of the i-, j-, and R-components, are shown in Fig. 2. The values of $\Delta(i\text{–}j)$ for the interactions $R1$–$X4$, $R2$–$X1$, $R1$–$X1$ (Fig. 2a), $X1$–$X1$ (Fig. 2b), and $X3$–$X4$ (Fig. 2c) are practically independent from r_R and are responsible for the relative size of the unit cell dimensions. In view of the change of the occupation mode of the $X4$ and $X1$ sites in the homogeneity range, the nonlinear slopes of the unit cell parameters in Fig. 1 can be connected with a partial ordered occupation of the $X1$ and $X4$ sites by Ag and Ga atoms.

The slope of the unit cell dimensions versus $r(R^{3+})$ is shown in Fig. 3. With increasing $r(R^{3+})$ the b and a-axes increase monotonically, but the value of the structure sensitive c-parameter decreases. This behavior may be also attributed to the occupation mode and to the change of interactions along this direction (see also above). For (Yb^{3+}) the unit cell dimensions for $Yb_3Ag_{3.8}Ga_{7.2}$ are not consistent with a linear slope in Fig. 3, which implies another

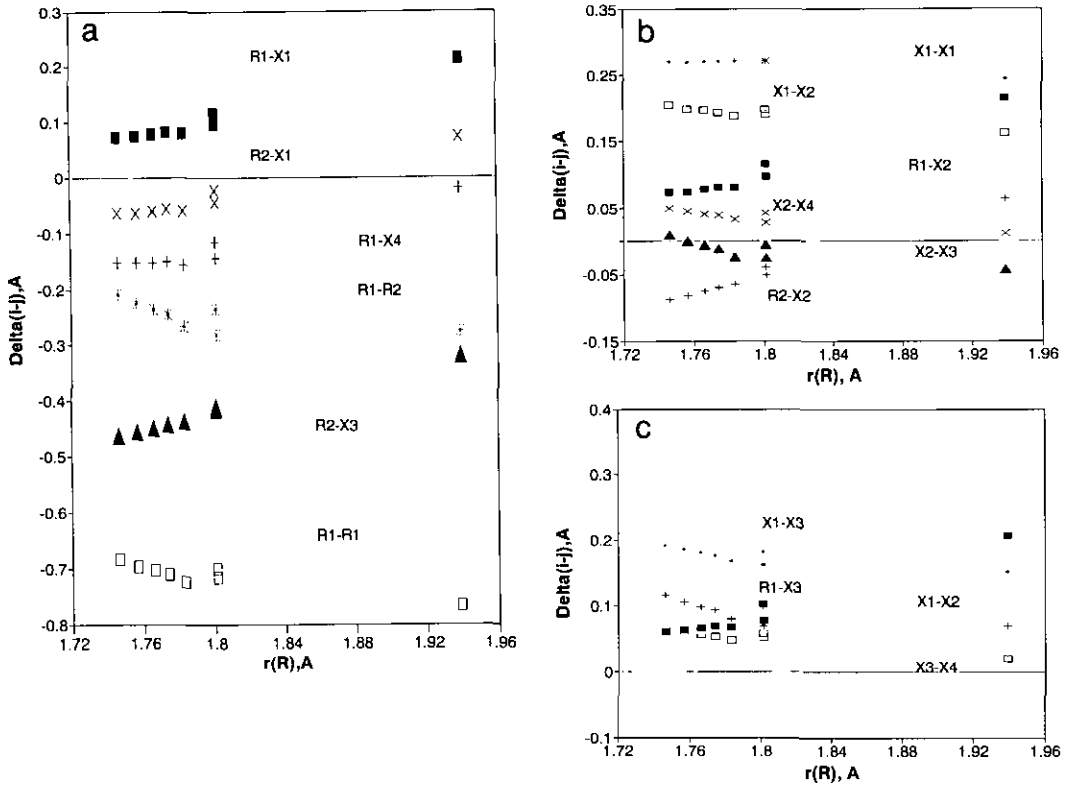

FIG. 2. Nearest neighbor diagram for $RE_3Ag_{3.8}Ga_{7.2}$: (a) values $\Delta(i-j)$ for the interactions $R1$–$X4$, $R2$–$X1$, $R1$–$X1$; (b) values $\Delta(i-j)$ for the interactions $X1$–$X1$, $R1$–$X2$, $X2$–$X3$; (c) values $\Delta(i-j)$ for the interactions $X1$–$X3$, $R1$–$X3$, $X1$–$X2$, $X3$–$X4$.

electronic state for ytterbium atoms than +3. The according values of the cell volume for Yb^{2+}, however, can be located on the linear graph as a strong indication of a +2 valence state of the ytterbium atoms (see also the section *Magnetism*).

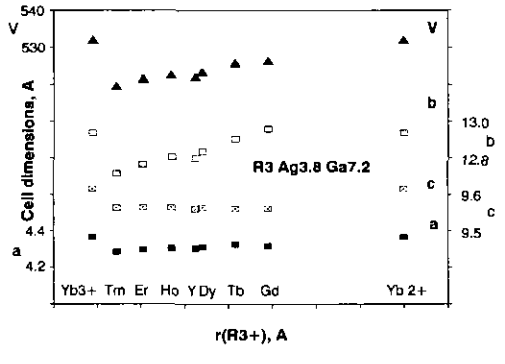

FIG. 3. Unit cell dimensions of $RE_3Ag_{3.8}Ga_{7.2}$ alloys versus radius of the rare earth ion.

Magnetism

The magnetic behavior of the $RE_3Ag_xGa_{11-x}$ alloys was investigated in the temperature range of 4 to 550 K. The magnetic data are presented in Table I as well as in Figs. 4 and 5.

$Y_3Ag_3Ga_8$ was found to be diamagnetic in the entire temperature range with a characteristic room temperature molar susceptibility $\chi_m = -1.2$ cm^3/mol.

The paramagnetism of the compounds (Gd, Tb, Dy, Ho, Er, Tm)$_3Ag_xGa_{11-x}$ closely obeys a Curie–Weiss law owing to a tripositive ground state of the rare earth atom. The effective paramagnetic moments and the corresponding paramagnetic Curie

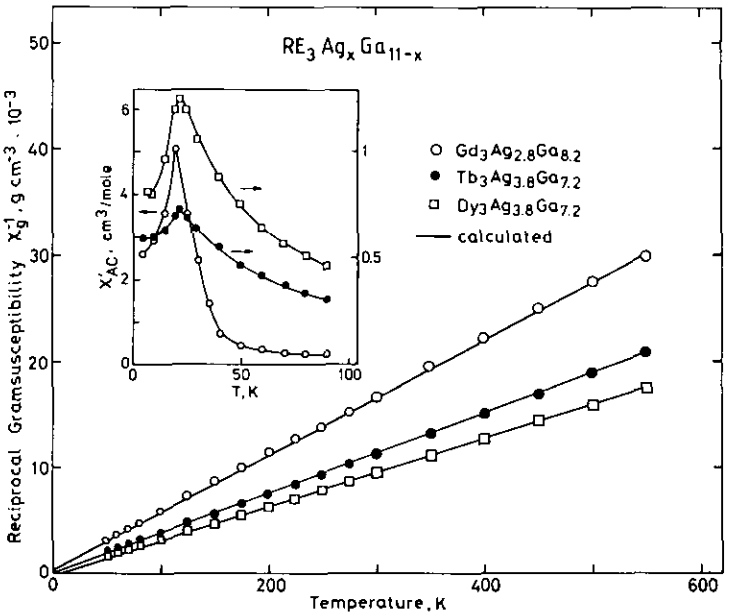

FIG. 4. Reciprocal gram-susceptibility versus temperature for $Gd_3Ag_{2.8}Ga_{8.2}$ and $(Tb,Dy)_3Ag_{3.8}Ga_{7.2}$. (Inset) Molar ac susceptibility below $T = 100$ K.

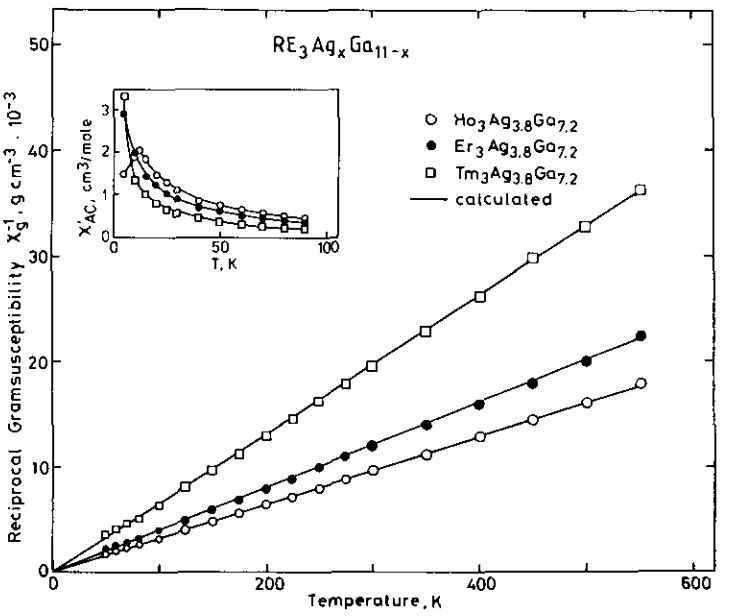

FIG. 5. Reciprocal gram-susceptibility versus temperature for $(Ho,Er,Tm)_3Ag_{3.8}Ga_{7.2}$. (Inset) Molar ac susceptibility below $T = 100$ K.

temperatures θ_p, as derived by least-squares fit according to the modified Curie–Weiss law, are listed in Table I.

When the temperatures are lowered, pronounced peaks in the susceptibility curves are encountered for the alloys with Gd, Tb, Dy, and Ho due to the onset of antiferromagnetic order of the rare earth sublattice. As the Néel temperatures approximately scale with the deGennes factor $J(J + 1)(g - 1)^2$, the RKKY indirect exchange interaction via the conduction electrons plays a major part in the coupling mechanism. Accordingly (Er or Tm)$_3Ag_xGa_{11-x}$ is expected to order magnetically below 4 K.

For the $Yb_3Ag_xGa_{11-x}$ alloys the Yb atom was found to be in a nonmagnetic Yb^{2+} ground state throughout the entire homogeneous range. The susceptibility is practically temperature independent paramagnetic down to 20 K. The upturns of the χ versus T curves below 20 K are obviously caused by small amounts of magnetic impurity phases as confirmed by slight deviations of the isothermal field dependency from linearity.

Acknowledgments

Yu. G. and M. E. thank Dr. K. Peters for the single crystal diffractometer measurements. Part of this research (H. K. and P. R.) has been sponsored by the Austrian Science Foundation FFWF under Grant P8218.

References

1. Z. Fisk and B. Maple, *J. Alloys Compounds* **183,** 303 (1992).
2. Yu. N. Grin, K. Hiebl, P. Rogl, and R. Eibler, *J. Less-Common Met.* **115,** 367 (1986).
3. Yu. N. Grin, P. Rogl, K. Hiebl, F. E. Wagner, and H. Noël, *J. Solid State Chem.* **70,** 168 (1987).
4. Yu. N. Grin, *Dopov. Akad. Nauk Ukr. RSR Ser. A* **2,** 76 (1982).
5. Yu. N. Grin, O. M. Sychevich, and O. R. Myakush, *Kristallografiya* **36,** 898 (1991).
6. L. G. Akselrud, Yu, N. Grin, and P. Yu. Zavalii, *in* "Collected Abstracts, 12th European Crystallographic Meeting, Moscow, USSR," Vol. 3, p. 155 (1989).
7. W. B. Pearson, *J. Less-Common Met.* **114,** 17 (1985).